

# Experimental and modeling study of hydrophobic associative polyacrylamide for enhanced oil recovery in carbonate reservoir

Saja Haider Mohammed<sup>1</sup>, Nizar Jawad Hadi<sup>2</sup>

<sup>1</sup>Department of Chemical Engineering and Petroleum Industries, Al-Mustaqbal University College, Iraq

<sup>2</sup>Department of Polymer and Petrochemical industries, Collage of Materials Engineering, University of Babylon, Iraq

## ABSTRACT

In this study, hydrophobic associative polyacrylamide (HAPAM) was used in conjunction with the chemical flooding technique in a low-permeability carbonates reservoir. To test the efficacy of the proposed method, both a model and an experiment were created. Experiments were run to compare the relative permeability (Kr) curves, oil recovery rates, and rheological, physical, aging time, and petrophysical features of brine water and polymer flooding in a core. The purpose of these tests was to show how HAPAM can be used to boost oil recovery. Computer Modelling Group (CMG), a simulator, was then used. An oil-and-brine (or HAPAM solution) grid in three dimensions (3D) was developed. The validity of the suggested simulator was established by comparing its results to those obtained from commercial software and from most of the brine or polymer flooding experiments. The developed simulator was used to undertake additional research into the non-Newtonian flow of brine or polymer solution in porous media. The experimental consequences indicated that the polymer solution has a shear thinning viscosity curve and flow behavior index. Shear thinning, viscosity, shear resistance, aging time, density, surface tension, and interfacial tension, and the water wet relative permeability curve are all improved by the adding 1500 ppm HAPAM to brine water. Moreover, oil recovery was about 80%. There was a strong agreement between the results of the modeling study and the experiments.

**Keywords:** Polymer flooding, Hydrophobic associative polyacrylamide, Rheological properties, Physical Properties, Petrophysical Properties, Core flooding test, and Computer Modelling Group (CMG).

### Corresponding Author:

Saja Haider Mohammed  
Department of Chemical Engineering and Petroleum Industries,  
Al-Mustaqbal University College, 51001, Hilla, Babil, Iraq  
E-mail: saja.haider@uomus.edu.iq

## 1. Introduction

As oil productivity rises, the need for water injection drops, and output rises, EOR techniques are gaining favor. In spite of its widespread use, water flooding loses its efficiency as a mobility ratio is unfavorable and a displacement efficiency is low; this is especially true when the oil has already been partially recovered. Production wells in the field are prematurely economically restricted due to high volumes of produced and injected water [1]. The goal of EOR is to reduce the quantity of oil that is left behind in reservoirs after they have been flooded with water or gas [2]. It is estimated that only one-third of the oil in a specified reservoir is extracted using traditional methods, making the other two-thirds an attractive target for EOR techniques [3]. Chemically enhanced oil recovery (CEOR) stands for a common technique for EOR that includes using a polymer, surfactant, or alkaline flooding [4]. Because it increases fluid viscosity and yields a superior mobility ratio [5], polymer flooding is a useful alternative strategy for decreasing water output. The possibility of oil production is increased and the water break through is postponed when the swept efficiency is higher [6]. However, the effectiveness of the polymer is questioned when high salinity and hardness formation water is

considered [7]. They can alter fluid dynamics, resulting in better reservoir fluid displacement. Most commonly used chemical approaches for controlling fluid mobility in oilfield reservoirs include polymer flooding applications [8]. In China, for instance, it has been used to produce almost 10 million tons of oil annually [9]. Most frequently employed are the synthetic water-soluble polymers polyacrylamide (PAM) besides hydrolyzed polyacrylamide (HPAM). It is assumed that PAM is the extensively employed technique [10] due to its low cost and risk. If you want to maximize oil recovery with worthy polymer injectivity at a minor price, polymer flooding operations require the right water viscosity to provide favorable mobility. As a PAM solution is pumped into a reservoir from an injection well, a polymer solution's viscosity will change because the flow velocity, which is proportional to shear rate, varies from the well-bore to a distance of a few hundred feet from the bore [11]. This shift in the rheological features for a polymer solution may be affected by temperature and salinity as the polymer ages [12]. Water hydrolyzes the amide clusters in the PAM structure, destroying the polymer [13]. As PAM matures, it becomes increasingly unstable due to exposure to divalent salts and high temperatures, two environmental conditions that have been the subject of numerous research [14]. NaCl is the most common dissolved salt in reservoirs [15], while MgCl<sub>2</sub> and CaCl<sub>2</sub> may also be present in smaller concentrations. Monovalent (NaCl) and divalent cation combinations also greatly reduce PAM viscosity [16-20].

As a result of these factors, the recommended temperature range for using polyacrylamide in seawater and brine during polymer flooding is 70–82 °C [20–24]. Recently, nanoparticles (NPs) were employed as an alternative approach to fix the EOR challenges [25-30]. NPs are special as a result of their small size and huge surface area. Switching between positive and negative charges on the surface of NPs [31-33]; altering the NPs' hydrophobicity, hydrophilicity, or amphiphilicity; and so on. To alter the rock's wettability [34], improve rheological properties [35], and lessen interfacial tension [36-38], NPs can be injected to EOR displacement fluids. The amount of polymer or surfactant that adheres to reservoir rock can also be decreased by using NPs [39-41]. In a similar vein, additional research has shown that introducing NPs into PAM can increase its thermal stability [42-44]. In this present work, (HAPAM) at different concentrations was mixed with brine water. Rheological, physical and petro physical properties were measured. Core flooding test to determine relative permeability for water, polymer and oil respectively (K<sub>rw</sub>, K<sub>rp</sub> and K<sub>ro</sub>) . In addition, oil recovery percentage. CMG was used to make comparison between rheological, Kr and oil recovery percentage.

## 2. Materials and Approaches

### 1.1. Polymer Solution Preparing

Copolymer of acrylamide (AM) and 2-acrylamido-2-methylpropane sulfonic acid (AMPS) as hydrophobic Associative polyacrylamide (HAPAM), molecular weight (207.247) g/mol, density (1.45) g/l from Sigma-Aldrich (St. Louis, MO, USA). Brine water with 20% ppm NaCl was prepared by dissolved NaCl on magnetic stirred for 10 min. Polymer solutions was prepared using a HAPAM (500, 1000, 1500 and 2000) ppm in brine water on magnetic stirrer for 30 min. The reservoir is carbonate core from Basra. Oil with viscosity (3.115) Cp and density (0.9993) g/l.

### 1.2. Rheological Property Measurement

Investigations into the apparent viscosity of HAPAM solutions considered concentration, temperature, shear resistance, shear rate, and aging time. By using a Brookfield cone-plate viscometer with a spindle: 41Z, the rheological characteristics were investigated. Shear viscosity and flow curve was studied under shear rate between (5-45) s<sup>-1</sup>. The samples were allowed to rest for (48) hours to examine their shear resistance qualities, viscosity was measure under 25 °C and shear rate 7.2 s<sup>-1</sup>. HAPAM solutions were aged chemically by being placed in an oven at 25, 50, and 65 °C for intervals of 2, 4, 10, 20, and 30 hours, respectively, while being sheared at a rate of 7.2 s<sup>-1</sup>. In other words, measurements taken immediately after food preparation have an ageing duration of zero. In particular, the viscosity results are well fit by a power law model depicted below:

$$\eta = K\gamma^{n-1} \quad (1)$$

K stands for the consistency index (Cp.sn<sup>-1</sup>),  $\eta$  represents a shear viscosity (cP),  $\gamma$  represents a shear rate (S<sup>-1</sup>), and n represents a flow behavior index (dimensionless).

### 1.3. Physical properties measurement

Density test has been performed by means of GP-120 S based on ASTM D-792 from China. The test made with different polymer solutions.

Surface tension was performed using JZYW-200B Automatic Interface Tensiometer provided through BEING UNITED TEST CO., LTD china. Check surface tension of polymer aqueous solutions in brine water at 25°C are made in contact with air. In addition, interfacial tension for polymer solutions in contact with crude oil also tested.

To determine the of ( $K_{rw}$ ,  $K_{rp}$  and  $K_{ro}$ ) fluid in carbonate core, polymer core flooding experiments were undertaken utilizing (HAPAM).

- 1- Core was cleaned by toluene and methanol, placed the core in a drying oven for 12 hours to dried it at 100 °C, saturated dried core by brine water for 21 days, weight after and before saturated, put inside accumulative filled by brine water and weighted again. The density of the core was calculated from the saturation water content.
- 2- At different injection rates, the core pressure was monitored as brine water was injected inside. The  $K_{rw}$  of cores was determined with the use of Darcy's law.
- 3- After the core had been fed HAPAM/brine water at a concentration of 1500 ppm under a flow rate of 6 cm<sup>3</sup>/min until the pressure reduction was stable,  $K_{rp}$  was calculated by repeating step 2. The subsequent equation explains the association between Darcy velocity and flow rate:

$$V_D = \frac{F_v}{A} \quad (2)$$

where A stands for a cross-sectional area of a core,  $V_D$  is the Darcy velocity, and  $F_v$  is the flow rate.

- 4 - At this point, having established  $K_{rw}$  in Step 2, crude oil was pumped into a core until it was completely saturated. When no brine water or polymer solution was created, the volume of brine water produced could be calculated along with the pressure drop across a core. An irreducible water saturation ( $S_{ir}$ ) has been computed. Absolute permeability, as defined by Darcy's law, refers to  $K_{ro}$  at  $S_{ir}$ .
- 5 - As shown in Figure 1, Exp. was carried out with brine water and polymer solution separately under predetermined injection rate after Step 4. The porosity, permeability and ( $K_{rw,p}$  and  $o$ ) curves was recorded. The Exp. was halted when no more oil was produced. The saturated and produced oil quantities were used to estimate the remaining oil saturation. The findings are summarized in Tables 3 and 4.

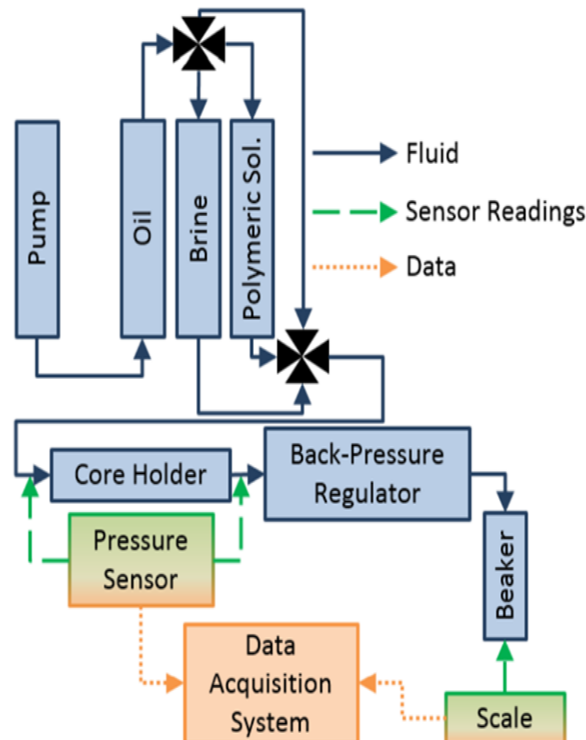


Figure 1. Core flooding test diagram [45]

#### 1.4. Simulation methodology

The simulation steps are as follows:

1. The reservoir initially consists of two phases: flooding with polymers or brine water and crude oil.
2. In the fundamental model, there is no allowance for free or solvent gas.

3. A grid-based core model without any geological heterogeneities or complexities is taken into consideration.
4. Radial fluid flow is minor in comparison to axial fluid flow.
5. No chemical reactions take place.
6. Oil, brine water, or polymer flooding obeys Darcy's Law when it flows through porous medium.

Table 1. Rock properties

Rock Properties	
Grid Size(x), cm	0.082
Diameter , cm	3.8
Length, cm	5.2
Grid	90
Permeability	45
Porosity, Ø %	20
Pressure, Psi	120
Temperature, °C	25
Rock Type	Carbonate

The CMG tool makes use of virtual representations of carbonate cores. Cartesians had to be constructed in order for a rectangular grid of 100 blocks to be created, each with a height of 5.2 cm and width of 3.8 cm, originally equal to the volume of a lab core. The STARS system model could be created by projecting the grid pattern in this manner. A numerical simulation of core flooding could be run using the actual core as input, which was transformed into a square cross-section. As a production end of the core was open to an atmosphere during core flooding, a bottom-hole pressure of 120 psi was employed in the numerical simulation model.

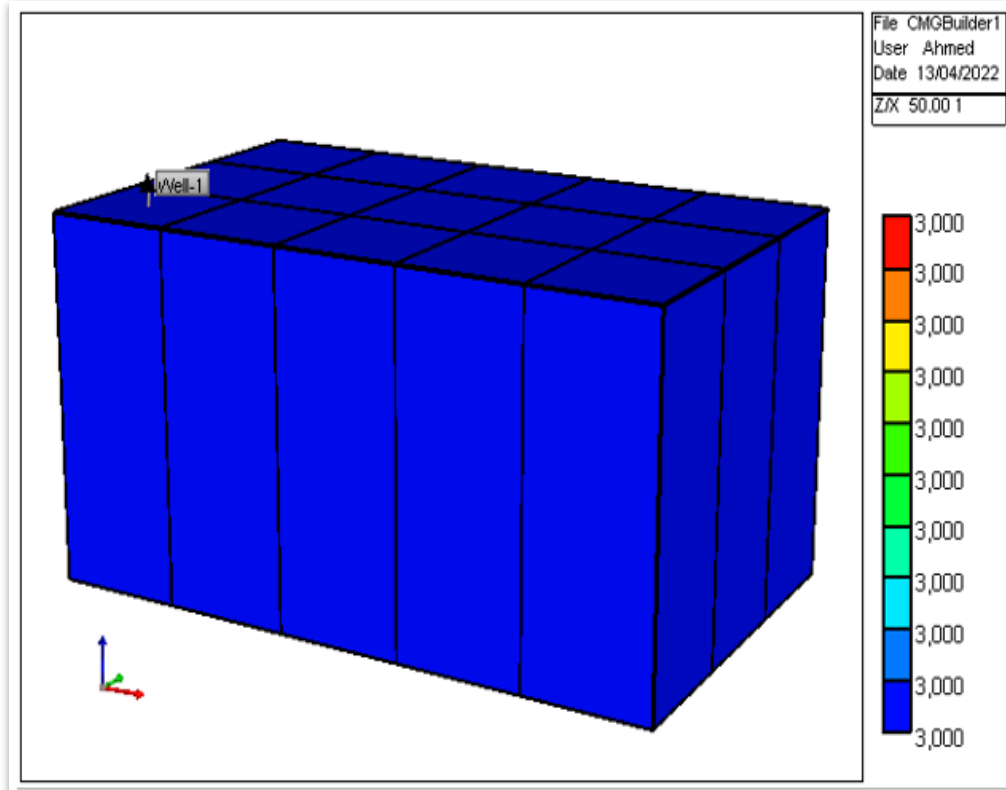


Figure 2. Cartesian grid pattern for flooding simulation

### 3. Result and discussion

Analyzing the correlation between shear viscosity and 500, 1000, 1500, and 2000 ppm HAPAM in brine water. As can be seen in Table 1, HAPAM viscosity rises as polymer concentrations rise up to around 1500 ppm, after which it begins to fall. This demonstrates the powerful viscosifying capabilities of HAPAM. In addition, it is

assumed that a concentration of 1500 ppm is optimal. In the case of HAPAM, increasing the concentration causes a decrease in viscosity by strengthening the surface-active properties for polymer solution, which in turn reduces the smallness of macromolecular chains [46].

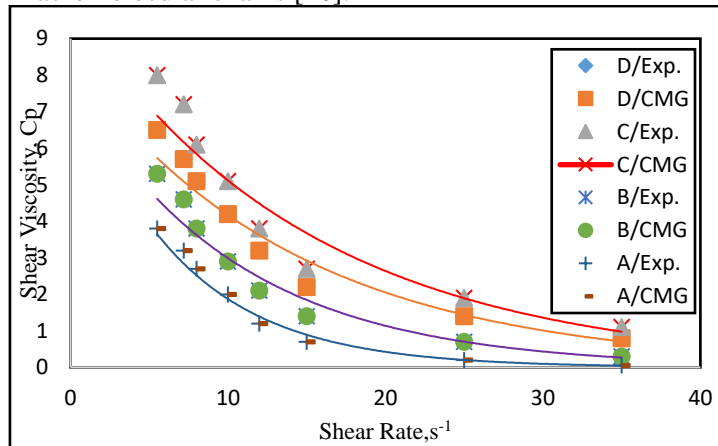


Figure 3. Experimental and modelling shear viscosity with shear rate of HAPAM/brine water at concentrations A:(500), B:(1000) ,C:(1500) in addition D:(2000) ppm at 25 °C

Figure 3 demonstrates how the viscosity of brine polymer solutions (A-D) significantly reduces as the shear rate increases. In contrast to A, B, and D, a shear thinning behavior of a brine solution with C is enhanced. Shear thinning was the prevailing tendency in all of the solutions at the (5–25) S<sup>-1</sup> range of shear rates. The measurements were found to be a worthy fit for the power law model equation 1 by means of the specified fitting factors in Table 1. Figure 2 displays the shear thinning behavior of high concentration solutions, which exhibited a larger slope than low concentration solutions. The index of flow behavior,  $n$ , is thus reduced as polymer concentration increases. The inverse is true for the consistency index  $K$ , as seen in Table 2. This occurs because of the substantial predicaments present in high concentration solutions. Since polymer molecules are more sensitive to enforced shear rates, which also reduce a degree of entanglements, minor viscosity with rising flow rates is the result [47]. The shear viscosity of a polymer increases as its molecular weight or concentration increases [48]. The viscosity of HAPAM, however, decreases with increasing concentration. When measured at a shear rate of 7.2 S<sup>-1</sup>, shear viscosities of A, B, C, and D brine solutions were 3.20, 4.60, 7.20, and 5.70 Cp, respectively. The shear rate considered to be appropriate for a reservoir determined by this work is 7.2 S<sup>-1</sup>. The rise in viscosity with Mw is responsible for an intensification in hydrodynamic volume and charge density for each molecule. However, the intensification in viscosity relating to concentration [49] might be attributed to the intensification in molecular density, which in turn increases the contact and repletion forces between negative charged polymer molecules. The consequences for the experimental investigation and the modeling study are in worthy conformity along this curve.

Table 2. HAPAM solutions characteristic

HAPAM Concentration (ppm)	Viscosity (cP)	Power law index $n$ , (dimension less)	Consistency index $K$ , (cP.s <sup>(n-1)</sup> )	Surface Tension	Interfacial Tension (mN/m)	Capillary Number
500	3.2	0.8	4.749	25.1	6.1	0.34
1000	4.6	0.66	8.316	25.5	5.7	0.51
1500	7.2	0.5	19.3119	27.7	3.8	1.15
2000	5.7	0.6	13.215	26.8	3.4	0.45

The shear resistance characteristics were evaluated after a second viscosity measurement was performed under the identical conditions. These consequences depict that the viscosities of HAPAM reverted to their original values (i.e., they held their viscosity even at increased shear rates and demonstrated pseudoplastic performance), which is indicative of a dynamic equilibrium between intermolecular association and dissociation. Hydrophobic chain introduced into a macromolecular backbone configuration of polyacrylamide, increasing its rheological properties [50]. Intramolecular/intermolecular hydrogen bonding and/or the hydrophobically correlating connections between the intra/intermolecular associations.

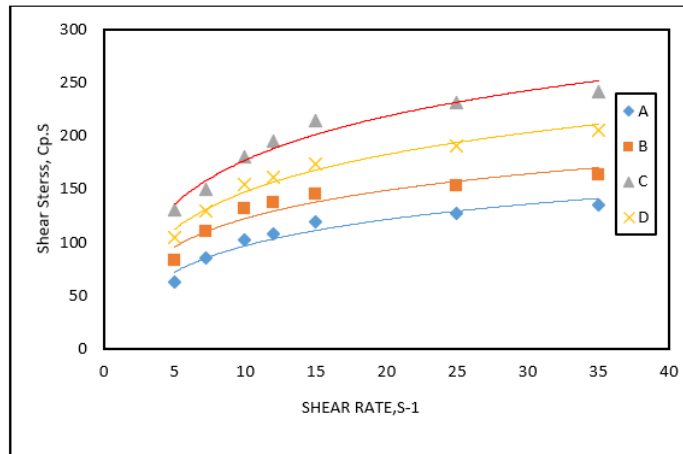


Figure 4. Shear stress with shear rate curves of HAPAM/brine water at concentrations A:(500), B:(1000), C:(1500) and D:(2000) ppm at 25 °C

The pseudoplastic behavior of the HAPAM polymer solutions, which is characteristic of a non-Newtonian fluid and frequently employed by chemical flooding agents [51], is evident in Figure 4. Since  $n = 0.5$  for the C solution indicated that since these fluids maintained their viscosity and strength despite being non-Newtonian (pseudo plastic), they are excellent EOR options for polymer flooding projects. The  $(n, k)$  values in table 1 were found to be in excellent agreement with those of [52] following linear fitting of the graph processing (equation 1).

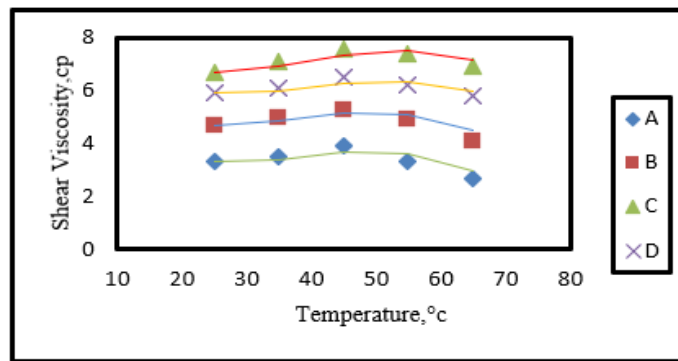


Figure 5. Effect of Temperature on Viscosity of HAPAM / brine Water at Concentrations A:(500), B:(1000), C:(1500) and D:(2000) ppm at shear rate  $7.2 \text{ S}^{-1}$

According to Figure 5, in HAPAM polymer solutions, viscosity progressively rises as temperature rises, reaches a peak at about  $45^\circ\text{C}$ , and then falls as temperature rises further. Because intermolecular hydrophobic association is an endothermic process with a rise in entropy, this can be partially attributable to the augmentation of intermolecular hydrophobic association with temperature [53].

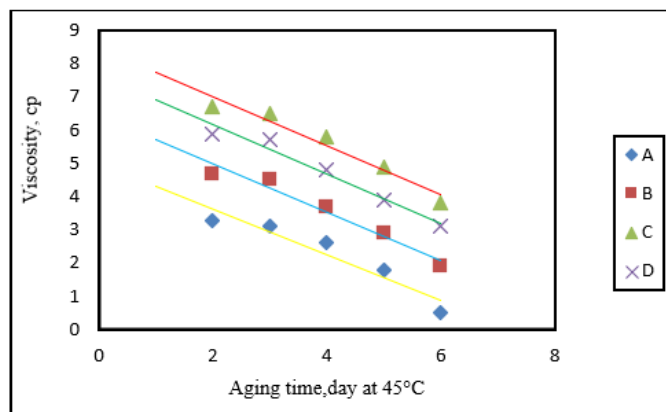


Figure 6. Relationship for an aging time with viscosity of HAPAM/brine water at concentrations (500,1000,1500 and 2000) ppm from A-D respectively

Figure 6 illustrates how viscosity changes as materials age. Viscosities of HAPAM solutions diminish to varying degrees as aging time increases. The viscosity of A is the highest, followed by B and D, while the viscosity of C is the lowest as aging time increases. The outcomes demonstrate that adding a hydrophobic group to HAPAM enhances its thermostability. The sulfonate group in HAPAM, on the one hand, increases the main chain stability and reduces the rate of HAPAM degradation [54]. In order to increase HAPAM associative polymer's stability in solution, adding a sulfonate group would be ideal because it would facilitate strong hydrogen bonding. The A-D polymer chain segment also shows the largest electrostatic repulsion since sulfonate is a potent electrolyte group. Viscosity is increased because of an electrostatic repulsion interaction, which causes a chain segment to stretch and produce uncoiled chains [55].

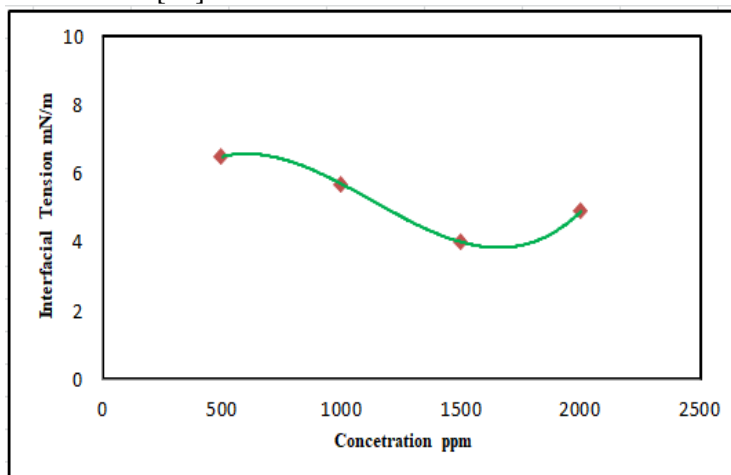


Figure 7. Interfacial tension curve of of brine solution mixed with HAPAM at concentrations A :(500), B: (1000) ,C: (1500) and D: (2000) ppm at 25 °C

Interfacial tension of oil and brine solution is lower than that of water and HAPAM (Figure 7). This is because their amphiphilic structure, which includes both hydrophilic and hydrophobic clusters, promotes intermolecular hydrophobic interactions and the creation of polymolecular micelles, both of which serve to decrease interfacial tension. The inclusion of hydrophobic clusters in the backbone configuration of the copolymer makes it possible for the molecules to clump together into aggregates or micelles, thereby decreasing their contact with water. They can also penetrate surfaces, which reduces the tension between the two layers of a material [56]. As a result, this HAPAM could be used into an EOR design as agents that lower interfacial tension to boost displacement efficiency in reservoirs located in high saline environments.

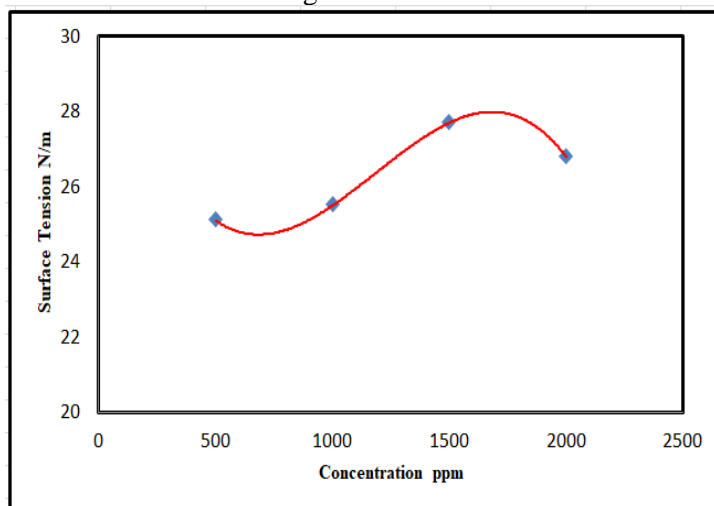


Figure 8. Surface tension curve of brine water / HAPAM at concentrations (500,1000,1500 and 2000) ppm at 25 °C

The surface tension increases with concentration (500,1000and 1500)ppm HAPAM as appear in Figure 8. After that decrease at 2000 ppm HAPAM/brine water began decrease as compared with other concentrations [57]. Density of HAPAM/ brine water increase with (500,1000 and 1500) ppm respectively as show in Figure 9. then 2000 ppm HAPAM/brine water density began decrease. High density referred by increase interlink ages between chains [58].



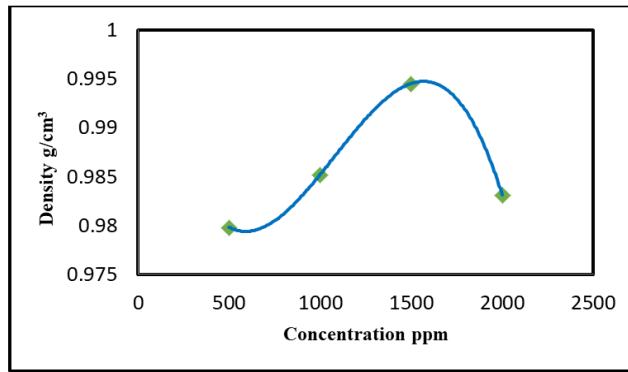


Figure 9. The density with concentration curve of brine water / HAPAM at concentrations (500,1000,1500 and 2000) ppm at 25 °C

Table 3. Petro physical properties

Core	Porosity (%)	Pore Volume (PV)%	Permeability (mD)		
			Ka	Kl	Ko
Carbonate	20	9.24	45	62.04	43.4

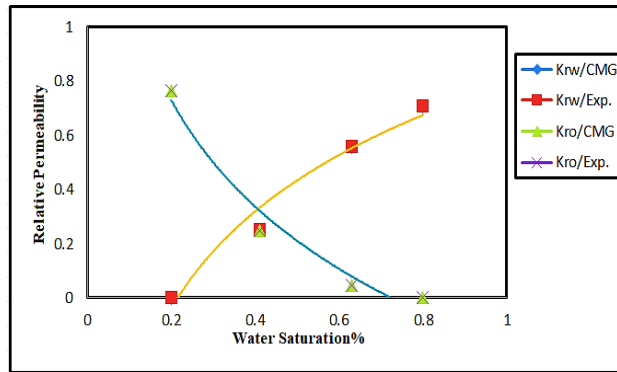


Figure 10. Relative permeability curve with water saturation for brine water flooding at A:(Krw/CMG), B:(Krw/Exp.),C:(Kro/CMG) and D(Kro/Exp.)

Figure 10, when brine water flooding is injected in carbonate core. The cross point of brine water relative permeability ( $k_{rw}$ ) with relative permeability of oil ( $k_{ro}$ ) appear less than 0.5. This occurs because the mobility ratio,  $M$ , for brine water is expected to be greater than one, indicating the presence of viscous fingering. The formation is confirmed to be oil-wet based on earlier justifications. This means that capillary forces limit water floods. The oil is stuck to the rock surface, and this adhesion forces water to flow backwards through the pores. Additionally, the oil contained within the reservoir has a very high viscosity. This results in the fingering water through the oil and trickle through a pores center [59].

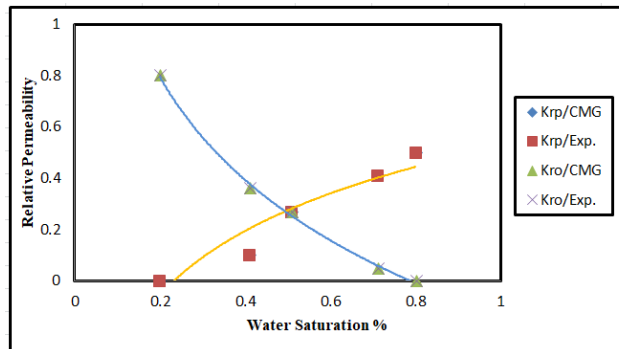


Figure 11. Relative permeability curve with water saturation for polymer flooding at A:(Krp/CMG), B:(Krp/Exp.), C:(Kro/CMG) and D(Kro/Exp.)



Figure 11, represent comparison between experimental and modelling study by CMG program. From this figure we show the degree of convergence between experimental and modelling study. Additionally, all of these cases had a flow rate of 6cc/sec. The fundamental parameters of core flooding experimentations have been listed in Tables 3 and 4. The mobility ratio is less than one and the polymer solution wets the porous media surface when the water relative permeability ( $k_{rw}$ ) besides oil relative permeability ( $k_{ro}$ ) intersect at a value less than 0.5. The 1500ppm HAPAM/brine water depicted in Figure 10 is a promising candidate for chemical tertiary recovery [58, 59] in a wet reservoir. Figure 2 shows how the actual core's circular cross-section was turned into a square cross-section with the similar cross-sectional area to aid in the development of a numerical simulation model of core flooding. Core flooding exposed a production end to atmospheric pressure; hence a minimum bottom whole pressure of 120 psi was used in the numerical simulation model.

Table 4. Oil recovery

Core Type	Solutions	Oil Recovery %	Additional Oil Recovery %	Saturation (%)		
				Swi	Soi	Sor
Carbonate	Brine water	40 at 99.95% water cut	-	9	91	60
	1500ppm HAPAM/brine water	80 at 99.99% water cut	40			20

#### 4. Conclusion

- 1- The flow of a polymer solution exhibiting shear thinning behavior at low shear rates was detected by researchers using a cone-plate viscometer.
- 2- As the HAPAM concentration increases from 500 to 1500ppm, the power law index  $n$  drops and the viscosity consistency  $K$  increases.
- 3- 1500 HAPAM/brine water give high viscosity, shear resistance, chemical aging time, density, surface tension and low IFT.
- 4- The relative permeability curves for brine water and polymer solution contain oil wet and water wet components, respectively. This conclusion is supported by experimental data and numerical result from CMG-STARS.
- 5- HAPAM solution flooding is a promising technique for chemical EOR. This is because, as compared to brine water flooding, it has been demonstrated to boost cumulative oil output.
- 6- The impacts of oil displacement efficiency were investigated using core flooding tests, which demonstrate that flooding with 1500ppm HAPAM/brine water performs significantly better than flooding with brine water alone.
- 7- Good agreement between experimental and modelling study.

#### Declaration of competing interest

The authors declare that they have no known financial or non-financial competing interests in any material discussed in this paper.

#### Acknowledgments

The authors would like to express their gratitude to the University of Babylon's Department of Polymer and Petrochemical Industries, College of Materials Engineering, and Al-Mustaqbal University College's Department of Chemical Engineering and Petroleum Industries for their contributions to this work. We would also like to thank everyone who helped make this endeavor a success.

**References**

- [1] S. Thomas, "Enhanced oil recovery-an overview," *Oil & Gas Science and Technology-Revue de l'IFP*, vol. 63, pp. 9–19, 2008.
- [2] V. Alvarado and E. Manrique, "Enhanced oil recovery: An update review," *Energies*, vol. 3, no. 9, pp. 1529–1575, 2010.
- [3] J. J. Sheng, *Modern chemical enhanced oil recovery: theory and practice*. Gulf Professional Publishing, 2010.
- [4] G. Moritis, "New technology, improved economics boost EOR hopes," *Oil and Gas Journal*, no. 16, 1996.
- [5] Y. Zhang, M. Wei, B. Bai, H. Yang, and W. Kang, "Survey and data analysis of the pilot and field polymer flooding projects in China," in *All Days*, 2016.
- [6] D. Wang, R. S. Seright, Z. Shao, and J. Wang, "Key aspects of project design for polymer flooding at the Daqing oilfield," *SPE Reserv. Eval. Eng.*, vol. 11, no. 06, pp. 1117–1124, 2008.
- [7] B. Wang, Y. Chen, S. Liu, H. Wu, and H. Song, "Photocatalytical visbreaking of wastewater produced from polymer flooding in oilfields," *Colloids Surf. A Physicochem. Eng. Asp.*, vol. 287, no. 1–3, pp. 170–174, 2006.
- [8] L. Shi, Z. Ye, Z. Zhang, C. Zhou, S. Zhu, and Z. Guo, "Necessity and feasibility of improving the residual resistance factor of polymer flooding in heavy oil reservoirs," *Pet. Sci.*, vol. 7, no. 2, pp. 251–256, 2010.
- [9] Y. U. Qiannan, L. I. U. Yikun, S. Liang, T. A. N. Shuai, S. U. N. Zhi, and Y. U. Yang, "Experimental study on surface-active polymer flooding for enhanced oil recovery: A case study of Daqing placanticline oilfield, NE China," *NE China. Petroleum Exploration and Development*, vol. 46, no. 6, pp. 1206–1217, 2019.
- [10] M. Jingwen *et al.*, "Determination and removal of PAM in oil-field wastewater," *INDUSTRIAL WATER TREATMENT-TIANJIN*, vol. 26, no. 3, 2006.
- [11] D. A. Z. Wever, L. M. Polgar, M. C. A. Stuart, F. Picchioni, and A. A. Broekhuis, "Polymer molecular architecture as a tool for controlling the rheological properties of aqueous polyacrylamide solutions for enhanced oil recovery," *Ind. Eng. Chem. Res.*, vol. 52, no. 47, pp. 16993–17005, 2013.
- [12] K. Lewandowska, "Comparative studies of rheological properties of polyacrylamide and partially hydrolyzed polyacrylamide solutions," *J. Appl. Polym. Sci.*, vol. 103, no. 4, pp. 2235–2241, 2007.
- [13] L. Xu *et al.*, "Synthesis and thermal degradation property study of N-vinylpyrrolidone and acrylamide copolymer," *RSC Adv.*, vol. 4, no. 63, pp. 33269–33278, 2014.
- [14] S. Wei *et al.*, "Preparation, characterization, and photocatalytic degradation properties of polyacrylamide/calcium alginate/TiO<sub>2</sub> composite film," *Polymer Composites*, vol. 37, no. 4, pp. 1292–1301, 2016.
- [15] N. Lai *et al.*, "A water-soluble acrylamide hydrophobically associating polymer: Synthesis, characterization, and properties as EOR chemical," *J. Appl. Polym. Sci.*, vol. 129, no. 4, pp. 1888–1896, 2013.
- [16] K. S. M. El Karsani, G. A. Al-Muntasheri, A. S. Sultan, and I. A. Hussein, "Impact of salts on polyacrylamide hydrolysis and gelation: New insights," *J. Appl. Polym. Sci.*, vol. 131, no. 23, 2014.
- [17] Y. Feng, B. Grassl, L. Billon, A. Khoukh, and J. François, "Effects of NaCl on steady rheological behaviour in aqueous solutions of hydrophobically modified polyacrylamide and its partially hydrolyzed analogues prepared by post-modification: Rheological behaviours of modified polyacrylamide and analogues," *Polym. Int.*, vol. 51, no. 10, pp. 939–947, 2002.

- [18] Q. Deng, H. Li, Y. Li, X. Cao, Y. Yang, and X. Song, "Rheological properties and salt resistance of a hydrophobically associating polyacrylamide," *Aust. J. Chem.*, vol. 67, no. 10, p. 1396, 2014.
- [19] D. Levitt, S. Dufour, G. A. Pope, D. C. Morel, and P. R. Gauer, "Design of an ASP flood in a high-temperature, high-salinity, low-permeability carbonate," in *All Days*, 2011.
- [20] Y. Ji, Q. Lu, Q. Liu, and H. Zeng, "Effect of solution salinity on settling of mineral tailings by polymer flocculants," *Colloids Surf. A Physicochem. Eng. Asp.*, vol. 430, pp. 29–38, 2013.
- [21] P. Mpofu, J. Addai-Mensah, and J. Ralston, "Temperature influence of nonionic polyethylene oxide and anionic polyacrylamide on flocculation and dewatering behavior of kaolinite dispersions," *J. Colloid Interface Sci.*, vol. 271, no. 1, pp. 145–156, 2004.
- [22] R. S. S. Seright, A. R. R. Campbell, P. S. S. Mozley, and P. Han, "Stability of partially hydrolyzed polyacrylamides at elevated temperatures in the absence of divalent cations," *SPE J.*, vol. 15, no. 02, pp. 341–348, 2010.
- [23] M. S. Kamal, A. S. Sultan, U. A. Al-Mubaiyedh, and I. A. Hussein, "Review on polymer flooding: Rheology, adsorption, stability, and field applications of various polymer systems," *Polym. Rev. (Phila. Pa)*, vol. 55, no. 3, pp. 491–530, 2015.
- [24] K. S. M. ElKarsani, G. A. Al-Muntasheri, A. S. Sultan, and I. A. Hussein, "Performance of PAM/PEI gel system for water shut-off in high temperature reservoirs: Laboratory study," *J. Appl. Polym. Sci.*, vol. 132, no. 17, 2015.
- [25] Y. Deng, J. B. Dixon, G. N. White, R. H. Loeppert, and A. S. R. Juo, "Bonding between polyacrylamide and smectite," *Colloids Surf. A Physicochem. Eng. Asp.*, vol. 281, no. 1–3, pp. 82–91, 2006.
- [26] L. N. Nwidee, S. Al-Ansari, A. Barifcani, M. Sarmadivaleh, M. Lebedev, and S. Iglauer, "Nanoparticles influence on wetting behaviour of fractured limestone formation," *J. Pet. Sci. Eng.*, vol. 149, pp. 782–788, 2017.
- [27] A. Karimi *et al.*, "Wettability alteration in carbonates using zirconium oxide nanofluids: EOR implications," *Energy Fuels*, vol. 26, no. 2, pp. 1028–1036, 2012.
- [28] A. I. El-Diasty and A. M. Aly, "Understanding the mechanism of nanoparticles applications in enhanced oil recovery," in *Day 2 Tue, September 15, 2015*, 2015.
- [29] E. Aliabadian, S. Sadeghi, M. Kamkar, Z. Chen, and U. Sundararaj, "Rheology of fumed silica nanoparticles/partially hydrolyzed polyacrylamide aqueous solutions under small and large amplitude oscillatory shear deformations," *J. Rheol. (N. Y. N. Y.)*, vol. 62, no. 5, pp. 1197–1216, 2018.
- [30] J. Yuan *et al.*, "Effects of various nanoparticles on the rheological properties of carboxylic cellulose nanofibers and the compound system's application in enhanced oil recovery," *Energy Fuels*, vol. 35, no. 14, pp. 11295–11305, 2021.
- [31] M.-A. Ahmadi, Z. Ahmad, L. T. K. Phung, T. Kashiwao, and A. Bahadori, "Evaluation of the ability of the hydrophobic nanoparticles of SiO<sub>2</sub> in the EOR process through carbonate rock samples," *Pet. Sci. Technol.*, vol. 34, no. 11–12, pp. 1048–1054, 2016.
- [32] M. S. Kamal, A. A. Adewunmi, A. S. Sultan, M. F. Al-Hamad, and U. Mehmood, "Recent advances in nanoparticles enhanced oil recovery: Rheology, interfacial tension, oil recovery, and wettability alteration," *J. Nanomater.*, vol. 2017, pp. 1–15, 2017.
- [33] G. Cheraghian, *Effects of nanoparticles on wettability: A review on applications of nanotechnology in the enhanced Oil recovery*. 2015.
- [34] R. Saha, R. V. S. Uppaluri, and P. Tiwari, "Silica nanoparticle assisted polymer flooding of heavy crude oil: Emulsification, rheology, and wettability alteration characteristics," *Ind. Eng. Chem. Res.*, vol. 57, no. 18, pp. 6364–6376, 2018.
- [35] L. M. Corredor, M. M. Husein, and B. B. Maini, "Impact of PAM-grafted nanoparticles on the performance of hydrolyzed polyacrylamide solutions for heavy oil recovery at different salinities," *Ind. Eng. Chem. Res.*, vol. 58, no. 23, pp. 9888–9899, 2019.

- [36] S. Frijters, F. Günther, and J. Harting, “Effects of nanoparticles and surfactant on droplets in shear flow,” *Soft Matter*, vol. 8, no. 24, p. 6542, 2012.
- [37] B. A. Suleimanov, F. S. Ismailov, and E. F. Veliyev, “Nanofluid for enhanced oil recovery,” *J. Pet. Sci. Eng.*, vol. 78, no. 2, pp. 431–437, 2011.
- [38] M. B. Khan, M. F. Khoker, M. Husain, M. Ahmed, and S. Anwer, “Effects of nanoparticles on rheological behavior of polyacrylamide related to enhance oil recovery,” *Acad. J. Polym. Sci.*, vol. 1, pp. 1–2, 2018.
- [39] M. A. Haruna, E. Nourafkan, Z. Hu, and D. Wen, “Improved polymer flooding in harsh environments by free-radical polymerization and the use of nanomaterials,” *Energy Fuels*, vol. 33, no. 2, pp. 1637–1648, 2019.
- [40] X. Sun, Y. Zhang, G. Chen, and Z. Gai, “Application of nanoparticles in enhanced oil recovery: A critical review of recent progress,” *Energies*, vol. 10, no. 3, p. 345, 2017.
- [41] A. Gbadamosi, R. Junin, M. Manan, A. Agi, and J. Oseh, “Nanotechnology Application in Chemical Enhanced Oil Recovery: Current Opinion and Recent Advances,” in *Enhanced Oil Recovery Processes-New Technologies. IntechOpen.*, 2019.
- [42] E. Aliabadian, M. Kamkar, Z. Chen, and U. Sundararaj, “Prevention of network destruction of partially hydrolyzed polyacrylamide (HPAM): Effects of salt, temperature, and fumed silica nanoparticles,” *Phys. Fluids (1994)*, vol. 31, no. 1, p. 013104, 2019.
- [43] W.-H. Chen, Y.-F. Wang, Z.-P. He, and M.-C. Ding, “Stability, rheology and displacement performance of nano-SiO<sub>2</sub>/HPAM/NaCl dispersion systems,” *J. Fuel Chem. Technol.*, vol. 48, no. 5, pp. 568–576, 2020.
- [44] B. Peng, J. Tang, J. Luo, P. Wang, B. Ding, and K. C. Tam, “Applications of nanotechnology in oil and gas industry: Progress and perspective,” *Can. J. Chem. Eng.*, vol. 96, no. 1, pp. 91–100, 2018.
- [45] O. P. H. Kwan, *Rheology and Flow Visualization of Polymeric Nanofluids in Reservoir Dead-End Pore Spaces (Master’s thesis)*. 2020.
- [46] Y. Feng, L. Billon, B. Grassl, G. Bastiat, O. Borisov, and J. François, “Hydrophobically associating polyacrylamides and their partially hydrolyzed derivatives prepared by post-modification. 2. Properties of non-hydrolyzed polymers in pure water and brine,” *Polymer (Guildf.)*, vol. 46, no. 22, pp. 9283–9295, 2005.
- [47] Z. Zhu, O. Jian, S. Paillet, J. Desbrières, and B. Grassl, “Hydrophobically modified associating polyacrylamide (HAPAM) synthesized by micellar copolymerization at high monomer concentration,” *Eur. Polym. J.*, vol. 43, no. 3, pp. 824–834, 2007.
- [48] J. Li, B. Yu, S. Sun, and D. Sun, “Study on an N-parallel FENE-P constitutive model based on multiple relaxation times for viscoelastic fluid,” in *Lecture Notes in Computer Science*, Cham: Springer International Publishing, 2018, pp. 610–623.
- [49] C. Zheng and Z. Huang, “Self-assembly and regulation of hydrophobic associating polyacrylamide with excellent solubility prepared by aqueous two-phase polymerization,” *Colloids Surf. A Physicochem. Eng. Asp.*, vol. 555, pp. 621–629, 2018.
- [50] L.-W. Meng, W.-L. Kang, Y. Zhou, Z.-W. Wang, S.-R. Liu, and B.-J. Bai, “Viscoelastic rheological property of different types of polymer solutions for enhanced oil recovery,” *J. Cent. S. Univ. Technol.*, vol. 15, no. S1, pp. 126–129, 2008.
- [51] T. F. Ogunkunle, B. A. Oni, R. O. Afolabi, A. S. Fadairo, T. Ojo, and O. Adesina, “Comparative analysis of the performance of hydrophobically associating polymer, xanthan and guar gum as mobility control agent in enhanced oil recovery application,” *J. King Saud Univ. - Eng. Sci.*, 2022.
- [52] P. Zhang *et al.*, “One factor influencing the oil-displacement ability of polymer flooding: Apparent viscosity or effective viscosity in porous media?,” *Pet. Sci. Technol.*, vol. 30, no. 14, pp. 1424–1432, 2012.

- [53] D. Zhu, L. Wei, B. Wang, and Y. Feng, "Aqueous hybrids of silica nanoparticles and hydrophobically associating hydrolyzed polyacrylamide used for EOR in high-temperature and high-salinity reservoirs," *Energies*, vol. 7, no. 6, pp. 3858–3871, 2014.
- [54] Y.-J. Guo *et al.*, "Solution property investigation of combination flooding systems consisting of Gemini–non-ionic mixed surfactant and hydrophobically associating polyacrylamide for enhanced oil recovery," *Energy Fuels*, vol. 26, no. 4, pp. 2116–2123, 2012.
- [55] Y. Feng, L. Billon, B. Grassl, A. Khoukh, and J. François, "Hydrophobically associating polyacrylamides and their partially hydrolyzed derivatives prepared by post-modification. 1. Synthesis and characterization," *Polymer (Guildf.)*, vol. 43, no. 7, pp. 2055–2064, 2002.
- [56] N. Dumelié *et al.*, "Characterization of electrodeposited calcium phosphate coatings by complementary scanning electron microscopy and scanning-transmission electron microscopy associated to X-ray microanalysis," *Thin Solid Films*, vol. 492, no. 1–2, pp. 131–139, 2005.
- [57] A. A. Hamouda, O. Karoussi, and E. A. Chukwudeme, "Relative permeability as a function of temperature, initial water saturation and flooding fluid compositions for modified oil-wet chalk," *J. Pet. Sci. Eng.*, vol. 63, no. 1–4, pp. 61–72, 2008.
- [58] Y. Liu *et al.*, "An inversion method of relative permeability curves in polymer flooding considering physical properties of polymer," *SPE j.*, vol. 23, no. 05, pp. 1929–1943, 2018.
- [59] C. Fabbri *et al.*, "Comparison of history-matched water flood, tertiary polymer flood relative permeabilities and evidence of hysteresis during tertiary polymer flood in very viscous oils," in *Day 2 Wed, August 12, 2015*, 2015.